Supplemental Data

Video Legends

Video 1 (related to Fig 1)

Time-lapse recording of GLUT4 vesicle trafficking in basal adipose cells expressing HA-GLUT4-GFP / HA-GLUT4-mCherry. Cells were transfected with 8ug/ml each plasmid and observed 24 h after transfection. Video represents 2 minutes of recording.

Video 2 (related to Fig 2)

Time-lapse recording of dynamic lateral movement of HA-antibody-labelled GLUT4 in the plasma membrane of live adipose cells. Endocytosis and internalization of HA-antibody from the cell surface was blocked with 2 mM KCN. HA-antibody was visualized using a secondary antibody conjugated with Alexa-594. Video represents 4 minutes of recording. Note a Brownian-like motion of faint HA-labelled in between the stationary clusters of GLUT4. The estimated diffusion coefficient of individual HA-spots was found to be K_d~1.2 $\mu m^2/s$.

Video 3 (related to Fig 3)

Time-lapse recording of cells expressing clathrin-GFP and HA-GLUT4-mCherry. Cells were transfected with 4 µg/ml each plasmid and observed 24 h after transfection. Note the existence of stationary patches of clathrin at the PM, and smaller, mobile clathrin-labelled compartments.

Video 4 (related to Fig 4)

Montage of two types of time-lapse recordings of clathrin events at and outside the clusters. Upper panel shows formation and lateral displacement of a newly-detached clathrin vesicle that carries away HA-GLUT4 labelled with HA-antibody. Lower panel shows event that was taking place away from the GLUT4 clusters. Note no change in HA-GLUT4 signal at the site of clathrin assembly. Cells were transfected with 4 ug/ml Clathrin-GFP and 4 µg/ml of HA-GLUT4 and observed 24 h after transfection.

Video 5 (related to Fig 5)

Time-lapse recording of cells expressing IRAP-pHluorin and HA-GLUT4-mCherry. Cells were transfected with 4 µg/ml each plasmid and observed 24 h after transfection. Fusion events were marked by a rapid increase of pHluorin fluorescence. The pHluorin tag resides in the acidic (pH~5) lumen of GSV and has very low fluorescence; upon opening of the fusion pore, pH in the fusing vesicle equilibrates with pH of external medium and pHluorin increases its fluorescence several fold. Video represents 2 minutes of recording.

Supplementary Figure Legends

Figure S1 (related to Fig 1)

(A) Stationary (green) and mobile (red) GLUT4 structures in the TIRF zone were segregated using time projection method. Overlay image shows that most of the movements of GLUT4 originated

from or nearby the stationary GLUT4 structures. Time projection image shows traces of mobile GLUT4 structures. See Video 1. Bar, 5 μm.
(B) Quantification of the relative amount of GLUT4 localized to stationary and mobile structures. Data shown are averages obtained from 20 cells in the basal (non-stimulated) state, from five independent experiments. Error bars represent SEM.

Figure S2 (related to Fig 2)

(A) Quantification of HA-GLUT4-GFP and HA-antibody fluorescence localized in the TIRF-zone shows that insulin stimulated both the accumulation of GLUT4 near PM and exposure of GLUT4 at the clusters on the cell surface. The average fluorescent signal was measured in the GLUT4-GFP and HA-antibody channels in 20 basal cells (hollow bars) and 20 insulin-stimulated cells (filled bars) in four independent experiments. Insulin on average resulted in a 2-fold increase of HA-GLUT4-GFP fluorescence (accumulation) and a 3-fold increase of HA-labeling (exposure). Error bars represent SD.
(B) Correlation of HA-GLUT4-GFP and HA-antibody signals reveals a significant amount of GLUT4 localized, but not exposed at the clusters in the basal state. A total of 2352 clusters was analyzed. The green line shows a linear fit of all the data points and shows a trend that larger clusters have higher HA-antibody labeling (R=0.41). The red line shows the maximum observed ratio of HA-antibody/HA-GLUT4-GFP signals, which supposedly represents the clusters with all HA-GLUT4-GFP molecules exposed/labeled by HA-antibody.
(C) Surface plots of HA-antibody fluorescence from magnified regions show the insulin-stimulated increase of cell-surface HA-antibody labeling and HA-GLUT4-GFP clusters. The intensity is color-coded.

Figure S3 (related to Fig 3)

(A) Colocalization of clathrin and GLUT4 in the TIRF-zone. Rat adipose cells were co-transfected with clathrin-GFP (green) and HA-GLUT4-mCherry (red), and imaged using multi-color TIRF microscopy. Some of the structures were mobile and thus represented GSV (see Video 3).
(B) Colocalization of clathrin with GLUT4 clusters at the cell surface. Cells expressing clathrin-GFP (green) and HA-GLUT4 (no fluorescent tag) were fixed and stained with HA-antibody (red) under non-permeabilized conditions.
(C) Colocalization of caveolin and GLUT4 in the TIRF-zone. Rat adipose cells were co-transfected with caveolin-GFP (green) and HA-GLUT4-mCherry (red), and imaged using multi-color TIRF microscopy.

Figure S4 (related to Fig 4)

Cumulative amount of HA-antibody uptake associated with clathrin-events at, and outside of, the clusters. Cumulative graphs were constructed using all detected decrements of HA-antibody fluorescence corresponding to the clathrin events associated with the clusters, as well as all the other clathrin assembly events outside the clusters. The decrements were calculated as the difference of the mean intensity of HA-antibody averaged for 10 frames before and after clathrin disappearance.

Figure S5 (related to Fig 5)

(A) Isolated rat adipose cells were transfected with the pH-sensitive probe IRAP-pHluorin (green) and HA-GLUT4-mCherry (red), and imaged using multi-color TIRF microscopy. Single exocytosis events were detected as spikes of IRAP-pHluorin fluorescence that reflected opening of the fusion pore and equilibration of the pH inside the lumen of the fusing vesicle. Images represent a time-

projection of the time-lapse stack of GLUT4-mCherry and IRAP-pHluorin channels. IRAP-pHluorin events in a montage are marked with white circles.
(B) Series of time-frames showing a characteristic fusion event detected with IRAP-pHluorin.
(C) IRAP-pHluorin radial intensity profile (red) for the vesicle fusion event shown in (B). Full width half maximum (FWHM) of the radial intensity profile was acquired from Gaussian fit (black).
(D) Time-course of FWHM was used to analyze post-fusion dispersal and lateral diffusion of IRAP. Slope of the curve acquired from linear fit (red) was used to calculate diffusion coefficient of IRAP in the plasma membrane.

Figure S6 (related to Fig 6)

(A) Kinetic model of GLUT4 recycling integrating fusion-based formation of GLUT4 clusters and their role in the regulation of endocytosis. GLUT4 assumed to be cycling between four GLUT4 quasi-compartments: GLUT4-storage vesicles (*C0)*, monomeric GLUT4 in the PM (*C1)*, clustered GLUT4 (*C2)*, and GLUT4 in endosomes (*C3)*. GLUT4 endocytosis is restricted to the clusters. K_1 - the rate of fusion with release; K_2 - rate of fusion with retention; K_R - rate of GLUT4 release from the clusters into the PM; K_C - rate of GLUT4 monomers joining clusters; K_e - rate of endocytosis; and K_3 - rate of sorting of GLUT4 from endosomes to GLUT4-strorage vesicles.
(B) Modeling of transient increase in the amount of GLUT4 fusion events in response to insulin. To take into account the kinetics associated with insulin signaling (AKT accumulation at PM) we substituted the K_1 and K_2 constants with a sigmoid function calculated as follows: $K_1(t) = {}^{ins}K_1 + ({}^{bas}K_1 - {}^{ins}K_1) * exp(-t/\tau)$, where ${}^{bas}K_1$ and ${}^{ins}K_1$ are steady-state values of K_1 in the basal and insulin-stimulated states and τ - is the characteristic time of AKT accumulation at the PM. Curves represent the model simulation with the different τ: 1.0 min (magenta), 2.0 min(red), 2.5 min(green), 3.0 min(blue), and 4.0 min (cyan). Black curve represents simulation with instant Akt recruitment. Best fit of experimental data was given by τ =2.5 min, see Fig.6.

Supplementary Experimental Procedures

Adipose Cell Preparation

Adipocytes were isolated from epididymal fat pads by collagenase (1 mg/ml) digestion. Following isolation, adipocytes were washed twice with Krebs-Ringer-Hepes (30 mM) buffer (pH 7.4) containing 1 % bovine serum albumin (BSA) (fraction V).

Electroporation

Isolated cells were washed twice with Dulbecco's modified Eagle's medium containing 25 mM glucose, 25 mM HEPES, 4 mM L-glutamine, 200 nM(−)-N^6-(2-phenylisopropyl)-adenosine, and 75 μg/ml gentamycin, and resuspended to a cytocrit of 40%. Electroporation was carried out in 0.4-cm gap-width cuvettes (Bio-Rad) using a T810 square wave pulse generator (BTX), with the total concentration of plasmid DNA in each cuvette adjusted to 4 μg/ml and 100 μg/ml of carrier DNA (sheared herring sperm DNA; Boehringer Mannheim). After applying three pulses (12 ms, 200 V), the cells were washed once in Dulbecco's modified Eagle's medium, pooled in groups of 5 cuvettes, and cultured at 37 °C, 5% CO_2 in Dulbecco's modified Eagle's medium containing 3.5% bovine serum albumin. Rat adipose cells were harvested 20 h post-transfection.

Glucose uptake measurement

Cells (5-10% suspension) were incubated at 37 °C with constant shaking in Krebs-Ringer-Hepes (30 mM) buffer (pH 7.4) with 1 % BSA (fraction V), 200 nM adenosine either without (basal) or with (insulin-stimulated) 100 nM insulin. Following an initial 30-min incubation period with or without insulin, [U-14C] glucose (3 μM) was added for 30 min and the reaction was terminated by

separating cells from media by spinning the suspension through dinonyl phthalate oil. To control for the effect of culturing we measured the glucose uptake in response to insulin, both in fresh isolated cells and cells cultured for 24 h. Insulin stimulated a 6-fold increase of the rate of glucose uptake in fresh adipose cells, and 3-fold in cells cultured for 24 h. This change in response was due to both an increased basal glucose transport as well as lowered insulin-stimulated uptake.

HA-antibody surface-binding assay

For measurement of surface-exposed HA-GLUT4 using immunoflourescence microscopy, cells in suspension were either fixed with 4% formaldehyde in phosphate-buffered saline (PBS) for 10 min, or incubated with 2 mM KCN to deplete ATP and inhibit GLUT4 recycling (Satoh et al., 1993). A monoclonal anti-HA antibody (HA.11, Berkeley Antibody Co.) was added at a dilution of 1:1000, and the cells were incubated for 20 min. Excess antibody was removed by washing the cells three times, and incubated with secondary antibody conjugated with Alexa-594 (Invitrogen) for 20 min. Since this assay can only be applied to transfected cells expressing HA-GLUT4, we also checked GLUT4 localization in both fresh and transfected cells using antibodies against endogenous GLUT4. We found no statistically significant difference between the density of GLUT4 structures at the plasma membrane (TIRF zone) in fresh cells and cultured cells, suggesting that GLUT4 clustering was not significantly affected by culturing of the cells.

Image analysis

Data acquired with a combination of TIRF and WF modes was processed to determine the vertical position of GLUT4 structures. Z-coordinates were calculated using background-subtracted fluorescence intensities measured in TIRF (F_{TIRF}) and WF modes (F_{WF}) as follows: $Z = -d*\ln(F_{TIRF}/F_{WF})$, where d is penetration depth of evanescent wave. F_{TIRF}/F_{WF} ratio was also used for analysis of GLUT4 vesicles fusion/fission events to distinguish changes in fluorescence signal due to lateral redistribution of GLUT4 within PM from vertical displacement of a vesicle in the TIRF-zone.

For analysis of HA-GLUT4-GFP exposure at the cell surface we analyzed HA-antibody fluorescence intensity in distinct puncta associated with clusters of HA-GLUT4-GFP molecules, as well as in between the puncta, where PM labeling with HA-antibody was relatively uniform. To do that we applied spatial filtering to remove peaks corresponding to puncta, and generated an image that was used to measure the background intensity of the HA-signal. Then this background image was subtracted pixel by pixel from the original image to generate an image containing only puncta, which was used next to calculate amount of HA-antibody fluorescence in clusters. It is important to note that the background fluorescence image resulting from HA-antibody labeling of cell surface was essentially free of out-of-focus component as there was no antibody present inside the cell, moreover the autofluorescence in the mCherry channel was negligible compared to the specific HA-antibody-Alexa-594 signal.

Analysis of fusion and fission events was carried out using localization and detection of transient change of fluorescent signal in the IRAP-pHluorin and Clathrin-GFP channels correspondingly. The identified events were analyzed for associated change in GLUT4-mCherry or HA-antibody fluorescence. To establish the order in which molecules of interest appeared at the site of fusion / fission, we analyzed the available history of the events, i.e. the time-course of fluorescent signal in each channel in the all proceeding frames.

Kinetic Modeling and Simulation

Based on established data, GLUT4 recycles among GSV, endosomes, and plasma membrane. Our data suggest that GLUT4 in the plasma membrane exist in two states, as monomers and clusters. To account for that, we propose a new model with four GLUT4 quasi-compartments (Fig. S6): C_0 is the fraction of GLUT4 in GSV; C_1 is the fraction of GLUT4 present as monomers in the plasma membrane; C_2 is the fraction of GLUT4 in clusters; C_3 is the fraction of GLUT4 in endosomes.
For simplicity, we have excluded the minor amounts of GLUT4 that can be present in other compartments and the peri-nuclear area (less than 4 %), and assume that the total amount of GLUT4 in the quasi-compartments is constant, i. e. $C_0+C_1+C_2+C_3=1$.

$$\begin{aligned} dC_0(t)/dt &= K_3*(1-C_0-C_1-C_2)-K_1*C_0-K_2*C_0 \\ dC_1(t)/dt &= K_1*C_0-K_c*C_1*C_2+K_r*C_2 \\ dC_2(t)/dt &= K_2*C_0+K_c*C_1*C_2-K_r*C_2-K_e*C_2 \end{aligned} \qquad \textbf{(1)}$$

where K_1 is the rate of fusion with release; K_2 is the rate of fusion with retention; K_r is the rate of GLUT4 release from the clusters into the plasma membrane; K_c is the rate of GLUT4 monomers joining clusters; K_e is the rate of endocytosis (according to our data, takes place only at the clusters); and K_3 is the rate of sorting of GLUT4 from endosomes to GSV.

Based on our data and published data we estimated the fraction of GLUT4 in GSV, monomers and clusters in basal steady-state. The rest of GLUT4 we assume to be in endosomal fraction. From our experimental data we have also estimated K_1, K_2 and K_e. The steady-state distribution of GLUT4 is determined by a system of three algebraic equations (2), from which we can estimate the unknown constants, K_r, K_c and K_3 (Table 1).

$$\begin{aligned} &K_3*(1-C_0-C_1-C_2)-K_1*C_0-K_2*C_0 = 0 \\ &K_1*C_0-K_c*C_1*C_2+K_r*C_2 =0 \\ &K_2*C_0+K_c*C_1*C_2-K_r*C_2-K_e*C_2 =0 \end{aligned} \qquad \textbf{(2)}$$

To calculate the kinetic transition in response to insulin, we numerically solved the set of differential equations (1) using 5th order Runge-Kutta Fehlberg method as initial value problem with parameters determined in the basal steady-state. To take into account the kinetics associated with insulin signaling (AKT accumulation at the PM) we substituted the K_1 and K_2 constants with a sigmoid function calculated as follows: $K_1(t)= {}^{ins}K_1+({}^{bas}K_1 - {}^{ins}K_1)*exp(-t/\tau)$, where ${}^{bas}K_1$ and ${}^{ins}K_1$ are steady-state values of K_1 in the basal and insulin-stimulated states and $\tau=2.5\ min$ - is the characteristic time of AKT accumulation at the PM (Gonzalez 2009). We assume that all other parameters remain relatively unchanged in response to insulin, and verify if the model can explain experimentally obtained GLUT4 distribution in insulin steady-state as well as the kinetics of transient increase of fusion events (Holman 1994). Fig. 6B shows that 60-fold increase of K1 and 2-fold increase of K2 is sufficient to produce a 3-fold increase in the surface exposed GLUT4. Moreover it shows a similar kinetics of GLUT4 redistribution that was measure by independent methods (Satoh 1993; Quon 1994) with cell reaching steady-state by 10-15min. This model also reproduces the transient increase in GLUT4 fusion events delivering GLUT4 to the cell surface (Fig. 5E and 6C). The relative frequency of the fusion events with release and retention can be estimated as $K_1(t)*C_0(t)$ and $K_2(t)*C_0(t)$ under assumption of the equal amount of GLUT4 delivered during each type of fusion.

Table 1. The parameters of the kinetic model and steady-state distrbution of GLUT4

	Basal steady state	Insulin steady state
C_0 (GSV)	0.75	0.25
C_1 (monomers in PM)	0.1	0.4
C_2 (clustered in PM)	0.1	0.2
C_3 (endosomes)	0.05	0.15
K_1	**0.002**	**0.12**
K_2	**0.04**	**0.08**
K_3	**0.63**	**0.63**
K_e	**0.315**	**0.315**
K_r	**0.025**	**0.025**
K_c	**0.4**	**0.4**

References

Gonzalez E., et al., Proc Natl Acad Sci U S A. 2009 April 28; 106(17): 7004–7009.
Satoh S., et al., J Biol Chem. 1993. 268(24):17820-9
Quon MJ., et al., Proc Natl Acad Sci. 1994. 91(12): 5587-91
Holman, G. D. and Cushman, S. W. 1994. *Bioessays* 16, 753-9.

Figure S1

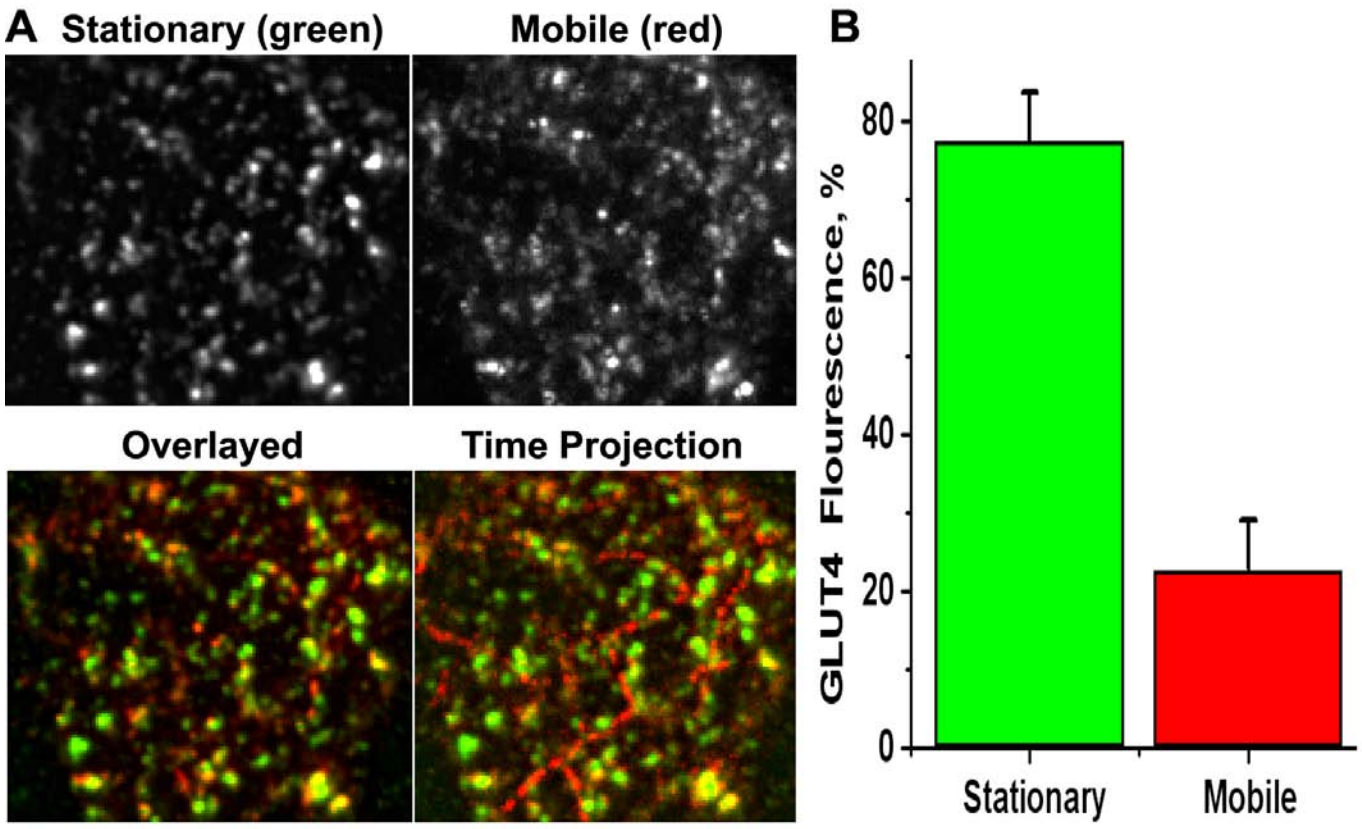
A
Stationary (green)
Mobile (red)
Overlayed
Time Projection
B
GLUT4 Flourescence, %
0
20
40
60
80
Stationary
Mobile

Figure S2

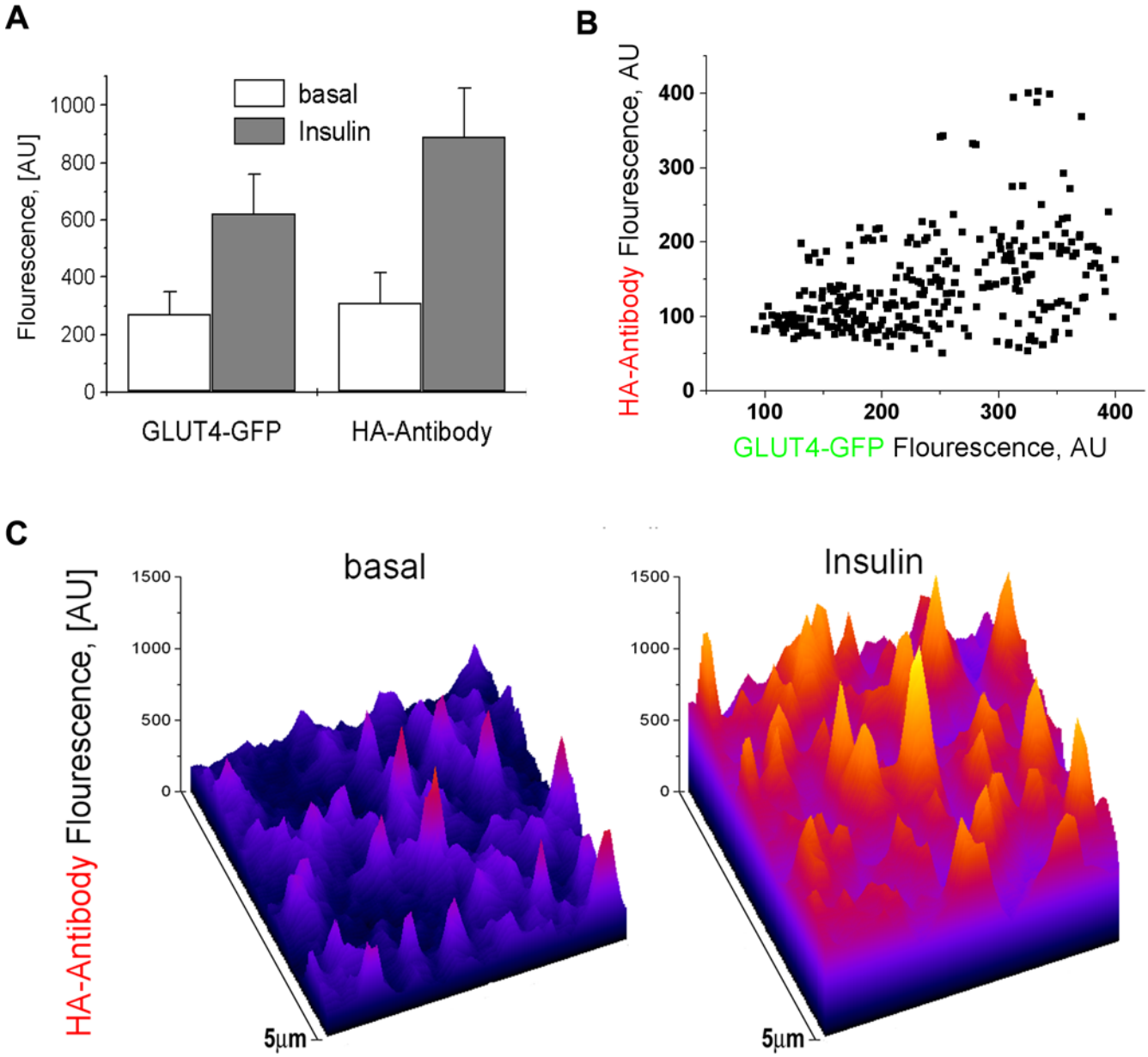
A
basal
Insulin
Flourescence, [AU]
1000
800
600
400
200
0
GLUT4-GFP
HA-Antibody
B
HA-Antibody Flourescence, AU
400
300
200
100
0
100
200
300
400
GLUT4-GFP Flourescence, AU
C
basal
Insulin
HA-Antibody Flourescence, [AU]
1500
1000
500
0
5µm

Figure S3

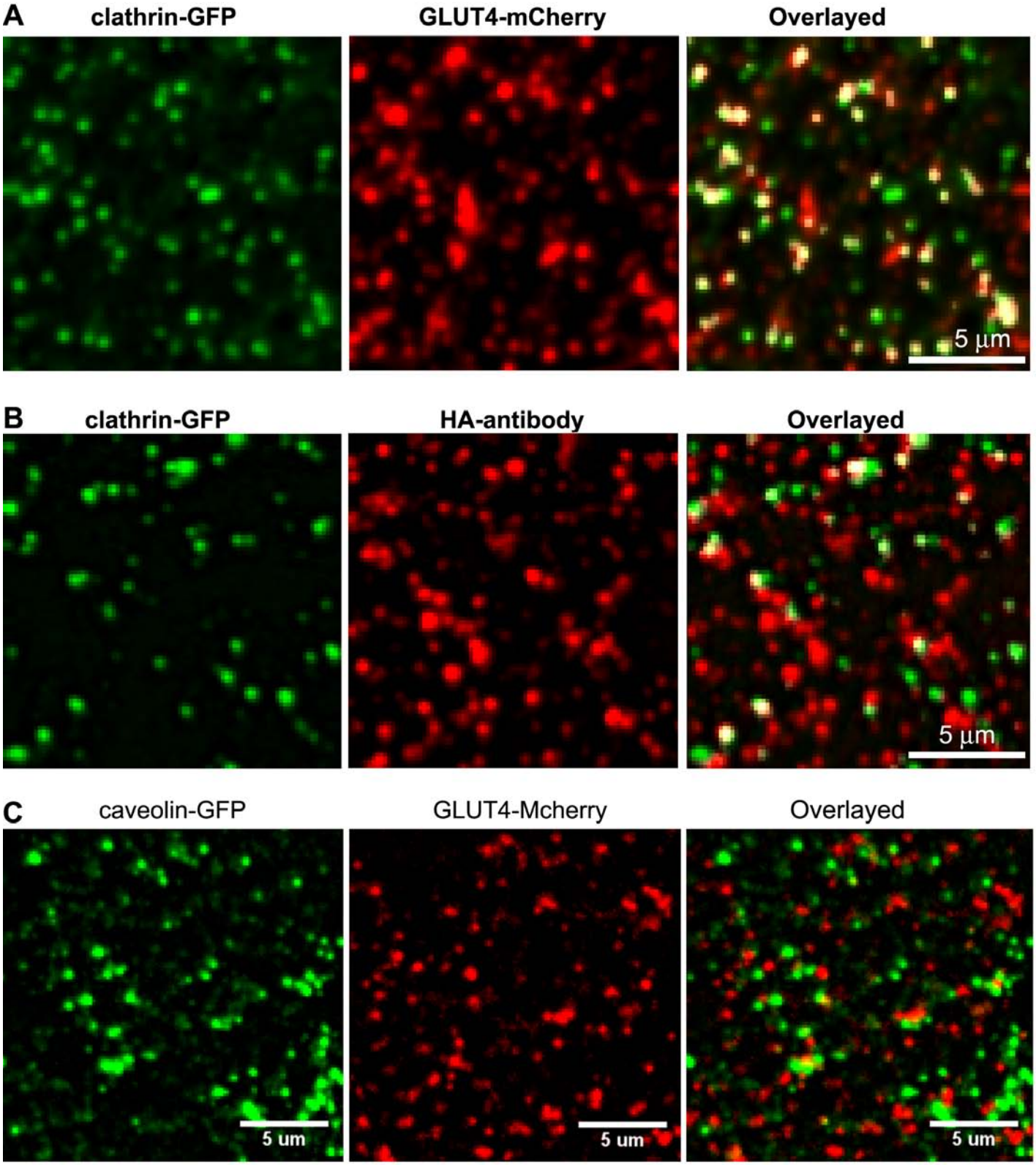
A
clathrin-GFP
GLUT4-mCherry
Overlayed
5 μm
B
clathrin-GFP
HA-antibody
Overlayed
5 μm
C
caveolin-GFP
GLUT4-Mcherry
Overlayed
5 um
5 um
5 um

Figure S4

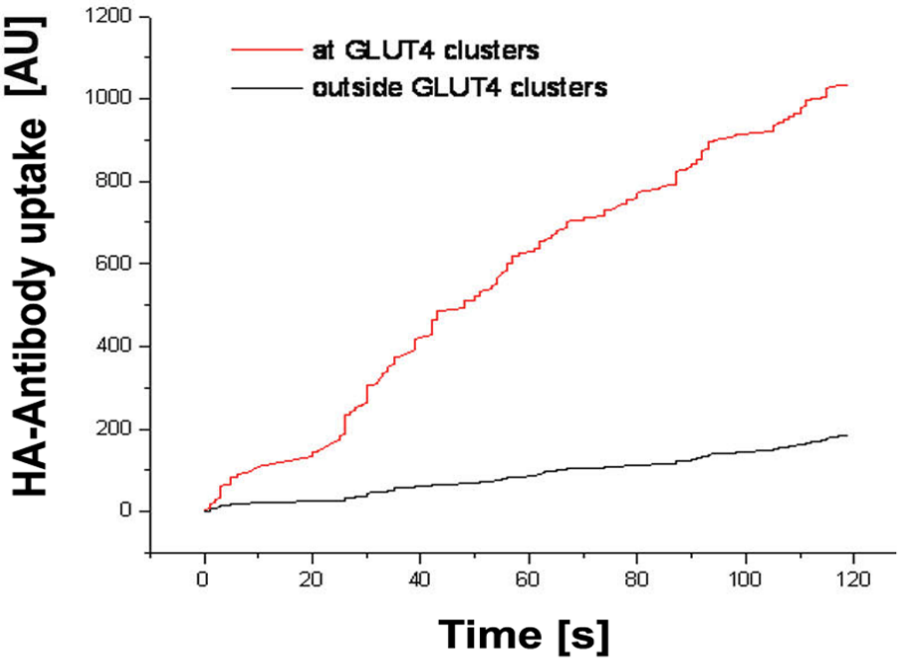
HA-Antibody uptake [AU]
1200
1000
800
600
400
200
0
at GLUT4 clusters
outside GLUT4 clusters
0
20
40
60
80
100
120
Time [s]

Figure S5

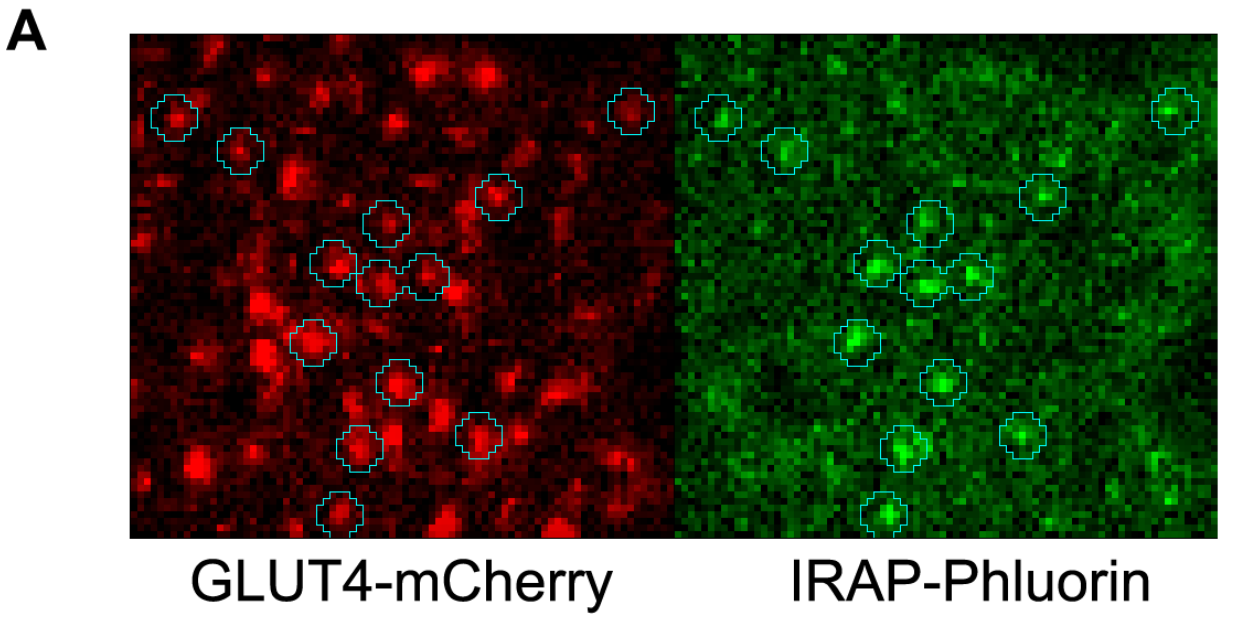
A
GLUT4-mCherry
IRAP-Phluorin
B
1.0 s
1.5 s
2.0 s
2.5 s
3.0 s
3.5 s
4.0 s
C
Pixel intensity [AU]
FWHM
distance [pixels]
D
Profile FWHM [μm²]
Time [s]

Figure S6

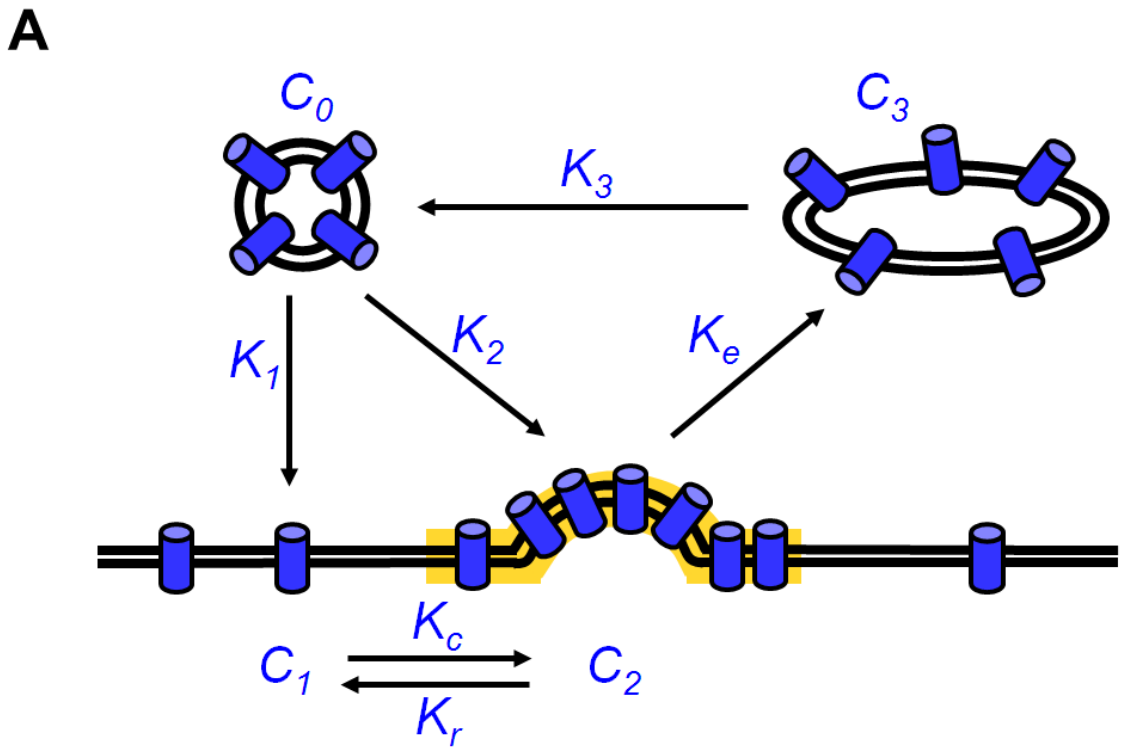
A
C_0
C_3
K_3
K_1
K_2
K_e
K_c
C_1
C_2
K_r

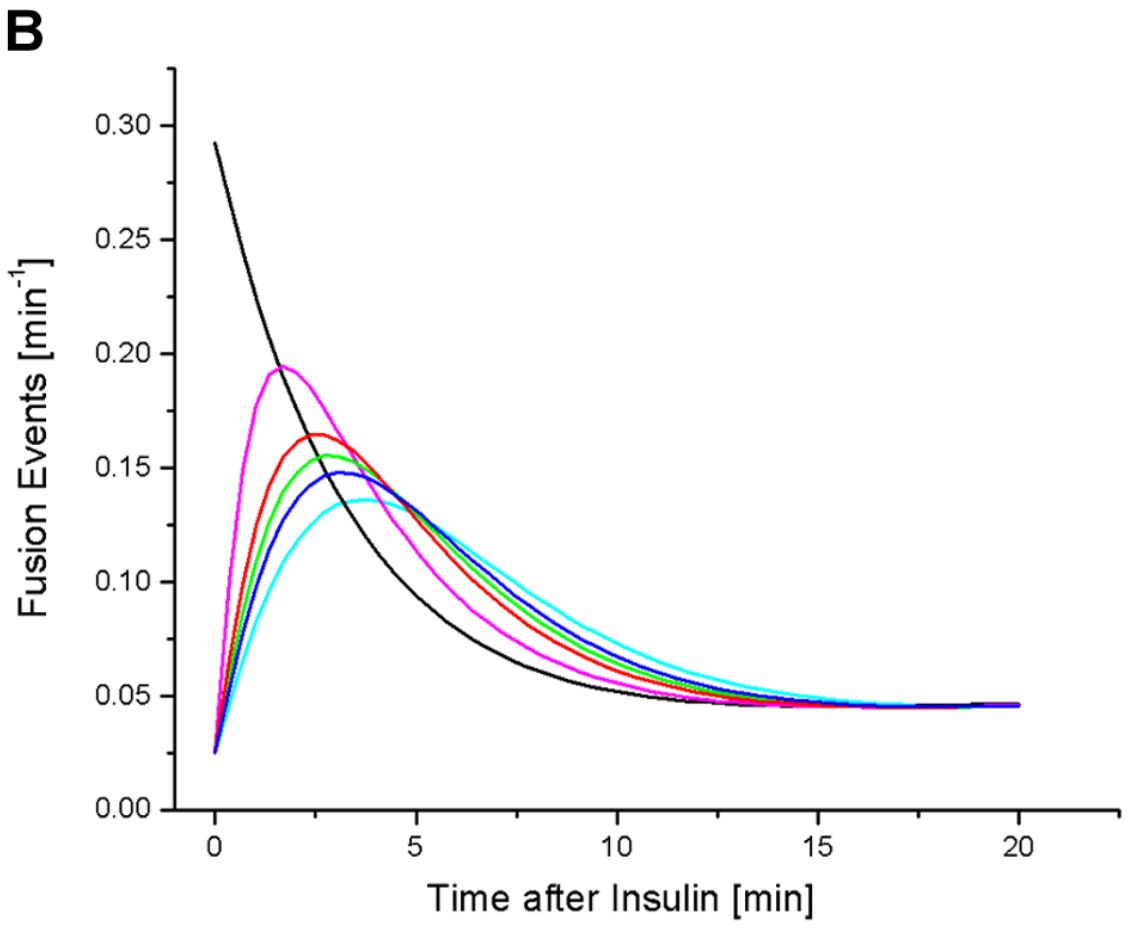
B
Fusion Events [min^{-1}]
0.30
0.25
0.20
0.15
0.10
0.05
0.00
0
5
10
15
20
Time after Insulin [min]